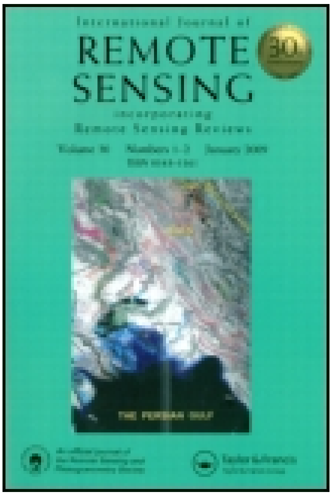

International Journal of Remote Sensing
Publication details, including instructions for authors and subscription information:
http://www.tandfonline.com/loi/tres20

Preliminary validation of ocean surface vector winds estimated from China's HY-2A scatterometer

Xiaofeng Yang[a], Guihong Liu[a], Ziwei Li[a] & Yang Yu[a]
[a] State Key Laboratory of Remote Sensing Science, Institute of Remote Sensing and Digital Earth of Chinese Academy of Sciences, Beijing 100101, China
Published online: 11 Jun 2014.

To cite this article: Xiaofeng Yang, Guihong Liu, Ziwei Li & Yang Yu (2014) Preliminary validation of ocean surface vector winds estimated from China's HY-2A scatterometer, International Journal of Remote Sensing, 35:11-12, 4532-4543, DOI: 10.1080/01431161.2014.916049

To link to this article: http://dx.doi.org/10.1080/01431161.2014.916049

International Journal of Remote Sensing, 2014
Vol. 35, Nos. 11–12, 4532–4543, http://dx.doi.org/10.1080/01431161.2014.916049

Preliminary validation of ocean surface vector winds estimated from China's HY-2A scatterometer

Xiaofeng Yang, Guihong Liu*, Ziwei Li, and Yang Yu

State Key Laboratory of Remote Sensing Science, Institute of Remote Sensing and Digital Earth of Chinese Academy of Sciences, Beijing 100101, China

(*Received 11 July 2013; accepted 4 December 2013*)

The microwave scatterometer on the Haiyang-2A (HY-2A) satellite is designed to provide global sea surface wind field data. The accuracy of HY-2A scatterometer wind retrievals is determined through various comparisons with moored buoys and the European Centre for Medium Range Weather Forecasting (ECMWF) reanalysis data. These comparisons were made in wide regions, including open sea and coastal areas, over a four-month period from January to March 2012 and August 2012. The retrieved wind speed results agree well with *in situ* observations and model data with respective biases −0.19 m s^{-1} and 0.01 m s^{-1} and root mean square error 2.02 m s^{-1} and 1.81 m s^{-1}. However, the wind direction errors are a little higher. The overall bias and root mean square deviation of wind direction are −2.24°, 1.74°, and 40.28°, 38.56°, respectively. The wind speed and direction residuals are higher in low- and high-wind speed ranges. In addition, the wind speed and direction are relatively more accurate for open sea than those in coastal regions.

1. Introduction

Since the first ocean observation satellite launched in the 1970s, space-borne scatterometers have provided valuable sea surface wind speed and direction estimates on synoptic scales. These ocean surface wind measurements obtained from scatterometers are widely used for various scientific and operational purposes. For example, the surface wind vector has been successfully used in enhancing numerical weather prediction models via data assimilation (e.g. Figa and Stoffelen 2000). Scatterometer wind observations have been used to predict and describe tropical cyclones in numerous studies (Katsaros et al. 2001).

The scatterometer (SCAT) on board the Haiyang-2A (HY-2A) satellite is a space-borne Ku-band radar instrument of China, which was launched in August 2011. The instrument is designed to accurately measure the radar backscatter from the surface of the earth. The backscatter over the ocean surface is primarily related to the wind speed and direction, and hence, ocean wind vector information can be inferred from the radar measurements.

The sea surface wind field obtained from HY-2A SCAT (e.g. Figure 1) is expected to enhance the sea forecasts and ocean storm warning. Such applications require the knowledge of the SCAT wind quality at various scales and the characterization of the related errors. Previous studies access the quality of scatterometer-derived wind, such as SeaSat/European Remote Sensing satellite (Freilich 1997), QSCAT/SeaWinds (Ebuchi, Graber, and Caruso 2002; Satheesan et al. 2007), ASCAT (Bentamy, Croize-Fillon, and Perigaud

*Corresponding author. Email: lgh422@gmail.com

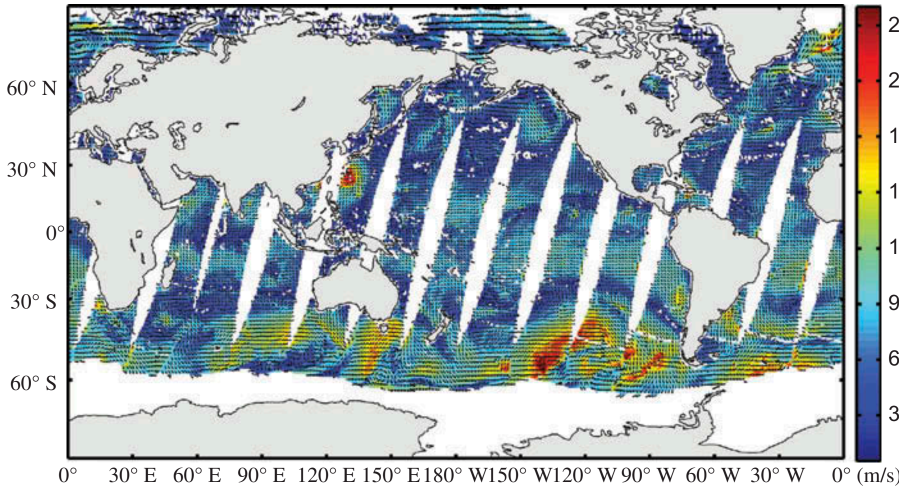

Figure 1. HY-2A scatterometer wind speed (m s^{-1}) and direction (°) retrievals occurring on 25 August 2012 (descending passes).

2008), and Oceansat-2 scatterometer (Singh, Kumar, and Pal 2012; Sudha and Rao 2013), comparing with *in situ* buoy observations, numerical weather prediction model wind products, or other scatterometer measurements. The aim of this article is to assess the accuracy and stability of the wind product retrieved from HY-2A SCAT measurements using a similar methodology by comparison with moored buoys and ECWMF reanalysis data.

2. Data preparation

2.1. HY-2A scatterometer winds

The HY-2A scatterometer is a Ku-band pencil-beam radar employing pulse compression techniques (Dong et al. 2004). It has a 1 m dish reflector antenna with two beams: the outer beam is VV-polarized and the inner beam is HH-polarized. As the satellite flies, each surface resolution cell can be viewed four times within the inner beam swath and twice within the outer beam swath: twice by the inner beam looking forward the aft, and twice by the outer beam (Wang et al. 2012).

HY-2/SCAT is a conically scanning scatterometer with fixed incidence angle for each polarization. Therefore, for each wind vector cell, the scatterometer measures sea surface radar backscatter from several azimuth angles. For the purposes of wind retrieval, a maximum likelihood estimation (MLE) method is implemented to retrieve possible wind vector pairs from different azimuth observation data (Lin et al. 2013; Chi and Li 1988). A brief description is presented below. The MLE objective function adopted by HY-2A to process the HY-2A scatterometer data is

$$J_{\mathrm{MLE}}(U,\Phi) = -\sum_{i=1}^{N}\left[\frac{(Z_i - M(U,\Phi-\phi_i,\theta_i,p_i))^2}{\Delta k} + \mathrm{In}\Delta k\right], \tag{1}$$

where

$$\Delta k = (V_{Ri})^{1/2} = (\alpha_i\ \sigma_i^{\ 2} + \beta_i \sigma_i + \gamma_i + V_{\varepsilon Mi})^{1/2}, \tag{2}$$

θ_i denotes incidence angle, U denotes wind speed, i represents the particular spatial location characterized by the radar polarization, and p_i polarization. $M(U, \Phi - \phi_i, \theta_i, p_i)$ is backscatter cross section calculated by the geophysical model function, z_i is a measurement value, $\Phi - \phi_i$ is the relative direction that is related to the radar azimuth angle Φ and the wind direction ϕ_i, $V_{\mathrm{R}i}$ is a function of the true value of σ_{0i}, and N represents the number of spatially and temporally collocated σ_0 measurements (σ_0 is the normalized radar cross-section of the sea surface, σ_{0i} is the value of σ_0 that would be measured by a perfect scatterometer instrument at the particular spatial location). Local maxima of J_{MLE} correspond to potential solutions.

The MLE approach is completely independent of the specific function form for the model function. A Ku-band geophysical model function (NSCAT-2) is used to relate the scatterometer backscatter section to ocean surface wind speed and direction (Wentz and Smith 1999). The wind retrieval algorithm aims to find the potential wind solutions that maximized the objective function for the given wind vector cell. Taking efficiency into account and starting with a given wind speed, a coarse ridge search is conducted first and then followed by an optimized wind solution based on the result of the coarse ridge search.

The wind retrieval processing above produces a set of potential solutions, which is known as 'ambiguities', for each wind measurement cell within the swath. The full set of ambiguous solutions can thus be thought of as a two-dimensional field defined on a cross-track, along-track grid. At each grid point (i, j), k is the number of the possible solution. An ambiguity removal algorithm based on a circular median filter is used to choose the best likely wind vector pair among the potential solutions (Schultz 1990). The filter is applied sequentially to each of the locations in the full field. After the filter has passed over all locations in the full field, the output median filter field $\phi_{ij}^{\ \mathrm{r}}$ replaces the initial field and the process is repeated until there is no further changes in the wind field or a set number of iterations are completed. The objective is to select the ambiguity $S_{ij}^{\ m}$, which is closest to the vector median $\phi_{ij}^{\ \mathrm{r}}$. At each point, the mth iteration of the wind vector, $S_{ij}^{\ m}$, is given by

$$\phi_{ij}^{\ \mathrm{r}} = MF(\phi_{ijk}\hat{E}k = S_{ij}^{\ m-1}, W_{ij}, N), \tag{3}$$

$$S_{ij}^{\ m} = min\left|\phi_{ijk} - \phi_{ij}^{\ \mathrm{r}}\right|, \tag{4}$$

where MF is a $N \times N$ median filter operator, and W_{ij} is the weighted vector median.

It is noted from the processing that the fully ambiguous vector field must be initialized before the median filtering is performed and there are two approaches. An obvious approach is to use the most likely wind vector pair as the initial field. The other is NWP model wind data. Here the latter is chosen. The global NWP data are interpolated in space and time to the locations of each HY-2A wind vector cell. The initial velocity solution at each location is chosen as the closest to the first- or second-ranked ambiguities to that direction.

2.2. NDBC buoys

In order to compare with HY-2A SCAT-derived vector wind data, observations from the buoys operated by National Data Buoy Center (NDBC) have been collected. Seventy-two buoy stations are identified. Among them, 39 buoys are near shore, and the other 33 are

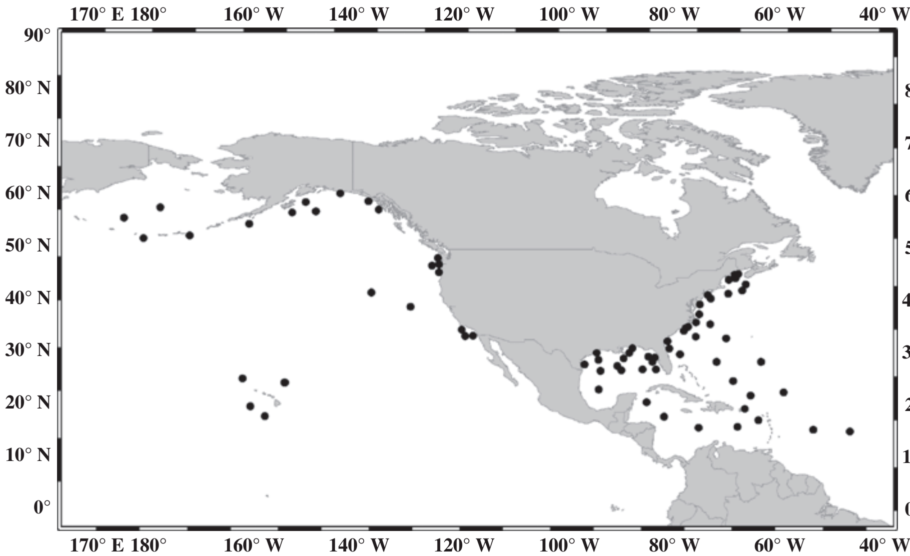

Figure 2. Map of the NDBC buoy locations used in the present study.

more than 200 km away from the land, considered representing offshore or open ocean conditions. Figure 2 shows the geographical locations of buoys used in this validation. The details of the buoys including instrument and stations are described in Meindl and Hamilton (1992). All historical buoy standard meteorological data are reported on the hour and represent eight-minute averages, so the time difference between satellite observations and buoy measurements is always within 30 minutes. Different NDBC moored buoys measure wind speed and direction at different heights (3, 5, and 10 m) due to different fleet types. All buoy wind speed data measured at different anemometer heights were adjusted to a reference level of 10 m using the log profile as follows.

$$U_{10} = 8.87403 \times U_z/\ln(z/0.0016), \tag{5}$$

where z is observation height in m, U_z is buoy wind speed measured at height z, and U_{10} is the 10 m wind speed.

2.3. ECMWF reanalysis

For the validation of HY-2A SCAT products, the ERA-interim reanalysis data used in this study have been obtained from the European Centre for Medium Range Weather Forecasting (ECMWF). These reanalysis data including zonal (u) and meridional (v) components of wind at 10 m height as well as data about atmospheric stability such as sea surface temperature, air temperature, and mean sea level pressure. It has a six-hourly temporal resolution (00, 06, 12, and 18 hours). It is made available on a regular grid of 0.5° × 0.5° in longitude and latitude.

3. Wind comparisons

3.1. Matchup data preparation

For the purpose of comparing coincident wind products, a triple temporal and spatial matchup data set is generated, which is from these HY-2A SCAT, buoys, and ECMWF reanalysis data. First, the temporal and spatial windows for the scatterometer measurement and a buoy observation were considered to be collocated if the distance between the centre of a wind vector cell and the buoy location and the differences in acquisition times were less than 30 minutes and less than 25 km, respectively. Then the selected buoys were used to match ECMWF data. ECMWF wind vector cells closest to the buoy locations in space and time were chosen. The temporal and spatial windows used for this collocation were limited to less than 1 hour and 0.5°, respectively. In order to avoid the reduction of residual errors caused by averaging SCAT data to ECMWF resolution, only pixels of SCAT that are closest to the ECMWF model grid centre are chosen to build the matchup data set.

3.2. Buoy comparisons

Surface wind vectors from HY-2A scatterometer are compared with NDBC moored buoys during the period from 1 January to 31 March 2012 and 1–31 August 2012. The comparison of HY-2A SCAT and buoys resulted in 4937 collocated measurement pairs. In general, the wind speed and direction derived by HY-2A SCAT agree well with buoy observations. The following section describes the validation results of HY-2A SCAT-derived wind field against buoys observation.

3.2.1. Comparison of wind speed and direction

Figure 3 shows the scatter diagrams of wind speed and direction comparisons observed by HY-2A SCAT and the buoys for all wind speed ranges in different regions. For moderate speeds (5–10 m s^{-1}), HY-2A SCAT data agree well with buoy observations. Our comparison shows a slight overestimation of wind speed by HY-2A SCAT at lower wind speeds (<5 m s^{-1}), and the wind speed from HY-2A SCAT is slightly underestimated at higher wind ranges (>10 m s^{-1}). This is also reflected by the statistics of the comparisons in Table 1. However, the wind direction data from HY-2A SCAT and buoys are symmetric, apart from a very small negative bias.

A more detailed analysis was carried out considering different limits of wind speed. Three different intervals are considered. The first one includes buoy wind speed 0–5 m s^{-1}, the second corresponds to values between 5 and 10 m s^{-1}, and the last one considers values higher than 10 m s^{-1}. Table 1 shows the root mean square error (RMSE) and bias calculated for these intervals using the HY-2A SCAT and buoy data in different areas. The overall RMSE in wind speed and direction are 2.02 m s^{-1} and 40.28° for the whole wind speed range, respectively. These statistics are considerably reduced to 1.68 m s^{-1} for speed and 33.83° in direction for the wind speed range 5–10 m s^{-1} with a slightly negative speed bias of −0.15 m s^{-1} and direction bias of −1.43°. However, a considerable increase in RMSE and bias for both wind direction and speed is observed during low (<5 m s^{-1}) and high (>10 m s^{-1}) wind speed ranges. This implies that the accuracy of the HY-2A SCAT-derived wind speed and direction at low- and high-wind speed range is worse than that at moderate-wind ranges. In addition, wind direction bias is more apparent for HY-2A SCAT winds at low-wind speeds than for moderate and high-wind speeds.

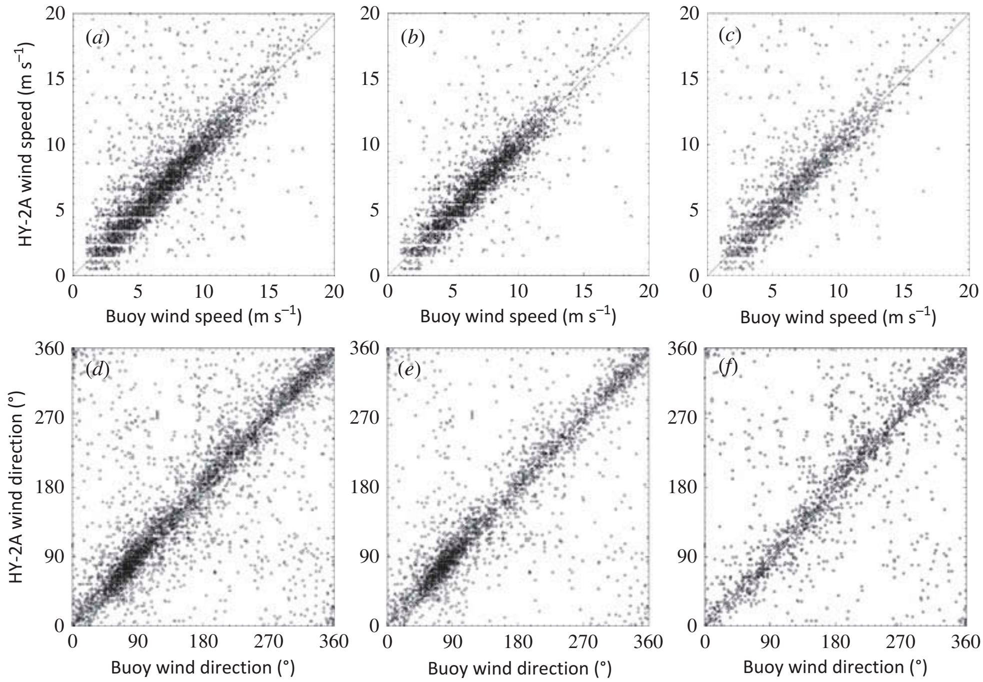

Figure 3. Comparison between HY-2A winds and buoy observations for all measured wind speed ranges and during January–March 2012 and August 2012. (*a*) and (*d*) are the comparison of all data, (*b*) and (*e*) in the open ocean, and (*c*) and (*f*) in the offshore area.

Table 1. Statistics of the comparisons of HY-2A SCAT and buoy observations during the period of January–March 2012 and August 2012.

Wind speed range ($m\ s^{-1}$)	Collocated number	Wind speed ($m\ s^{-1}$)		Wind direction (°)	
		Bias	RMSE	Bias	RMSE
Whole					
All	4937	−0.19	2.02	−2.24	40.28
<5	1304	−0.48	2.36	−3.03	53.44
5–10	2827	−0.15	1.68	−1.43	33.83
>10	806	0.11	2.43	−3.86	37.31
Open sea					
All	3246	−0.08	1.75	−1.89	33.53
<5	762	−0.29	1.85	−0.41	44.41
5–10	1994	−0.05	1.42	−1.78	28.92
>10	490	0.10	2.61	−4.57	32.18
Coastal					
All	1691	−0.40	2.46	−2.75	53.65
<5	542	−0.75	2.94	−4.60	68.45
5–10	833	−0.38	2.19	−1.39	46.04
>10	316	0.14	2.11	−3.25	43.46

In the open ocean, the error statistics demonstrated that the accuracy of HY-2A SCAT sea surface wind retrieval is apparently improved with the RMSE in wind speed and direction 1.75 m s^{-1} and 33.53°. In contrast, the accuracy is found to degrade near the shore region with the RMSE increasing to 2.46 m s^{-1} and 53.65°. The wind speed bias in the coastal areas is approximately −0.23 m s^{-1} as compared with −0.29 m s^{-1} in the noncoastal areas. This may result from the microwave backscatter signal being contaminated by the near-shore land through the side-lobe antenna pattern.

3.2.2. *Analysis of residuals*

Figure 4 shows the dependencies of residuals (Buoy-HY2A) of wind speed and direction on buoy wind speeds. Data were binned into 1 m s^{-1} intervals of buoy wind speed. Figure 4 illustrates the comparisons of wind speed and direction residuals with buoy winds for the whole region, and Figures 5 and 6 for the open sea and coastal region, respectively. A negative wind speed residual for HY-2A SCAT-derived winds is discernible with respect to buoy wind speed for low-wind speeds (<5 m s^{-1}), and the residual gradually shifts towards positive values as the wind speed increases. For higher wind speeds (>14 m s^{-1}), the speed residual is large and varies between positive and negative deviation. For the buoy wind speed range from 5 to 15 m s^{-1}, the wind direction residuals with most points are almost zero and show no systematic dependence on the buoy wind speed. From these figures, it also can be seen that the wind direction is less accurate, the RMSE increases for buoy wind speed <5 m s^{-1}, and the highest variations are observed for higher wind speeds (>15 m s^{-1}). In fact, it is difficult to retrieve the wind direction in low-

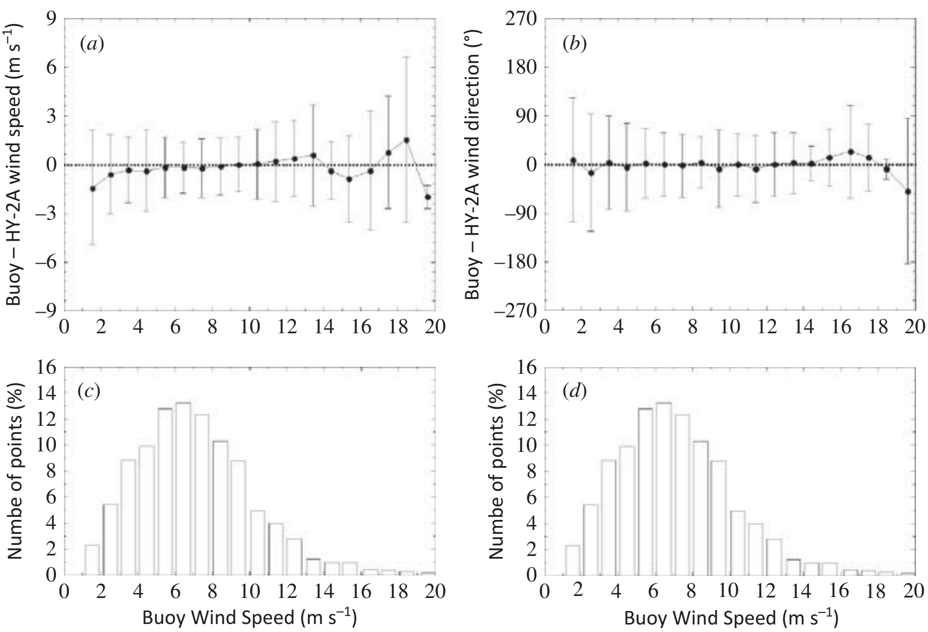

Figure 4. Dependence of wind direction and wind speed differences (buoy – HY-2A) on buoy wind speed. The point symbol in the upper panel represents the average of the differences based on 1 m s^{-1} bins, and the vertical line represents the one standard deviation. The bars in the lower panel show the histogram of data number.

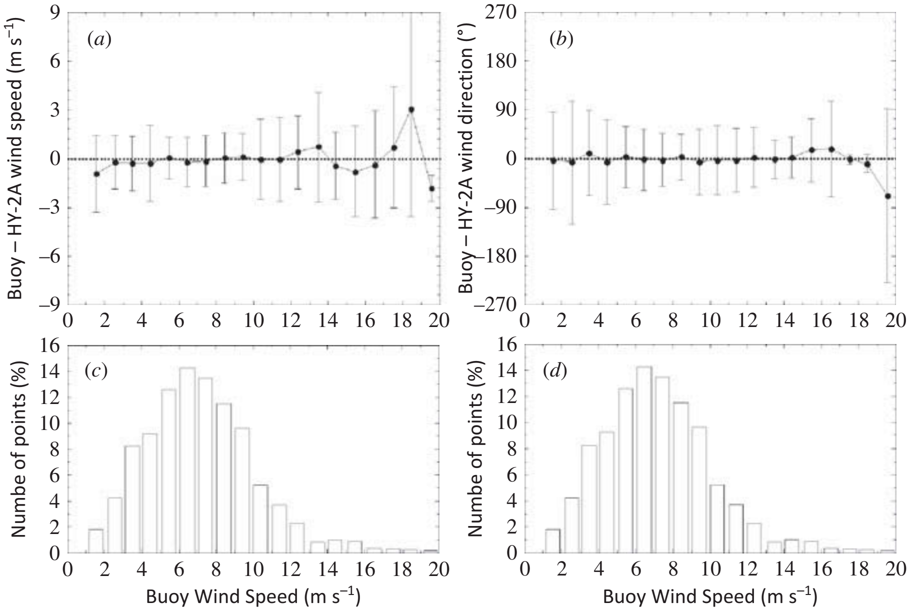

Figure 5. As in Figure 4 but for the open sea area.

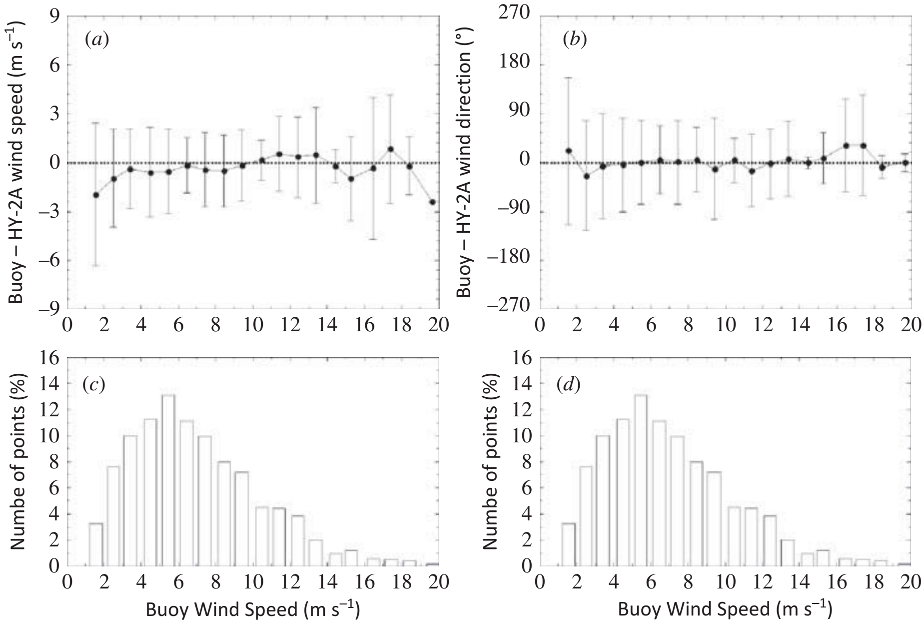

Figure 6. As in Figure 4 but for the coastal area.

wind speed. This is possibly due to the very low upwind/crosswind modulation of the backscattered power (Ebuchi, Graber, and Caruso 2002). In addition, the method used for direction ambiguity removal works poorly at low-wind speed (Ebuchi, Graber, and Caruso

2002). While high-wind speed conditions are usually associated with bad weather conditions, which can cause buoys motion as well as surface layer distortion (Large, Morzel, and Crawford 1995) or rain-contaminated scatterometer observations and therefore buoy measurements become less reliable. These features are apparently not only in the open sea but also in the coastal areas, except that the wind speed residual is larger for the coastal areas than the open sea.

3.3. ECMWF reanalysis comparisons

In this study, ECMWF reanalysis data are collected to validate the wind product derived from HY-2A SCAT. Figure 7 shows the scatter diagrams of the comparison between HY-2A SCAT and ECMWF data, and the detailed statistics of the comparison are given in Table 2. The overall results show that both comparisons (HY-2A SCAT-buoy and HY-2A SCAT-ECMWF) follow a similar behaviour for wind speed and direction. For the wind speed range from 5 to 10 m s^{-1}, the bias in both wind speed and direction is slight while the remarkable inconsistency in speed and direction can be observed in the collocated data pairs for the low (< 5 m s^{-1}) and high (>10 m s^{-1}) wind speed ranges.

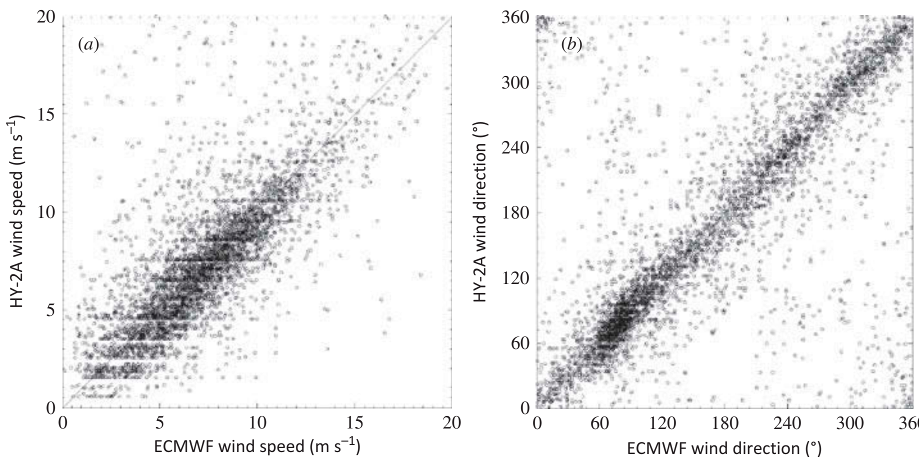

Figure 7. Comparison between HY-2A and ECMWF reanalysis data during January–March 2012 and August 2012.

Table 2. Statistics of the comparisons of HY-2A SCAT and ECMWF reanalysis during the period of January–March 2012 and August 2012.

Wind speed range (m s^{-1})	Collocated number	Wind speed (m s^{-1})		Wind direction (°)	
		Bias	RMSE	Bias	RMSE
All	4937	0.10	1.81	1.74	38.56
<5	1203	−0.42	1.78	4.44	50.29
5–10	2848	0.20	1.68	0.22	33.52
>10	886	0.48	2.07	3.11	35.87

The overall comparison shows that wind from HY-2A SCAT and ECMWF data are in good agreement with a bias of 0.10 m s^{-1} and an RMSE of 1.81 m s^{-1} in wind speed, considering all the collocated data. In the comparison of wind direction, the bias and RMSE are 1.74°38.56° for all the data and the lowest errors are 0.22° and 33.52° for the wind speed range 5–10 m s^{-1}.

The wind speed and direction variability were analysed considering the differences between HY-2A SCAT and model data. Figure 8 shows the residual (HY-2A SCAT-ECMWF) dependence on model wind speed. Data were binned into 1 m s^{-1} intervals of model wind speed. No significant differences are seen in the nature of dependence of the residuals on wind speed. It can be seen that for low-wind conditions, the speed residual is negative, indicating that HY-2A SCAT is overestimating, while it is underestimating for high-wind speed cases. The mean and standard deviation indicate that the residuals for winds in the range of 5–10 m s^{-1} are minimal, while for lower and higher ends they are larger. The HY-2A SCAT estimated wind direction for lower and higher wind speeds shows higher variations from model data than those with a moderate wind speed.

In addition, the distribution of residual in wind speed and direction with latitude is investigated, as shown in Figure 9. It was found that basically the differences in wind speed and direction between the two sources are not latitude dependent.

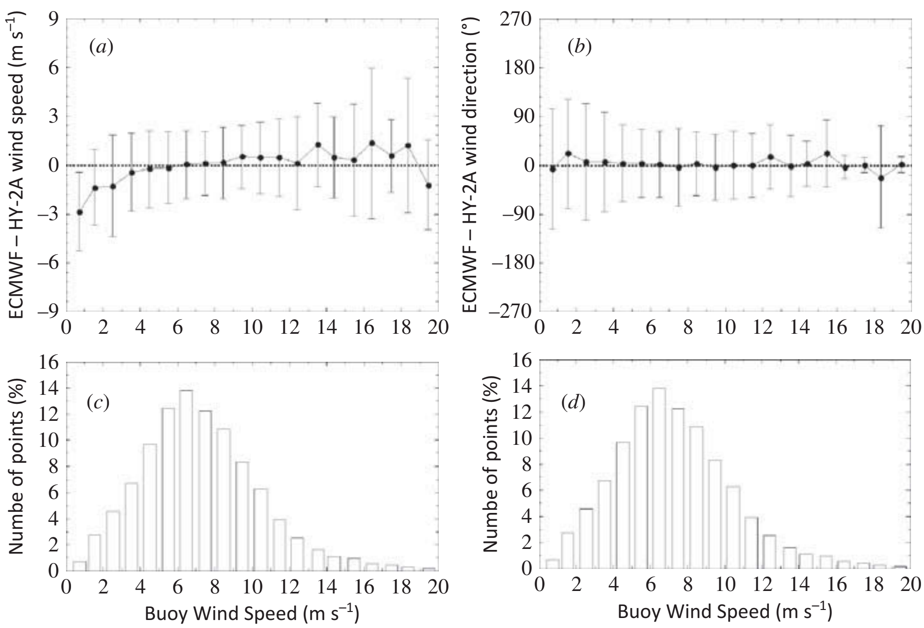

Figure 8. Dependence of wind speed and direction residuals (HY-2A SCAT-ECMWF) on the model wind speed. The point symbol in the upper panel represents the average of the differences based on 1 m s^{-1} bins, and the vertical line represents one standard deviation. The bars in the lower panel show the histogram of the data number.

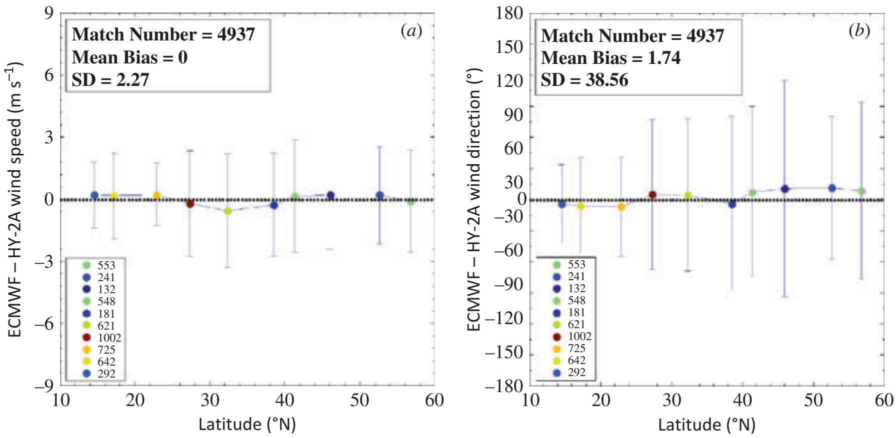

Figure 9. Dependence of wind speed and direction residuals (HY-2A SCAT-ECMWF) on the latitude. The colour points and bar in the panel represent the averages and standard deviations calculated in each 5° latitude interval.

4. Conclusion

The HY-2A SCAT wind observations are validated through a comparative analysis with collocated measurements from moored NDBC buoys, including offshore and open sea, and ECMWF wind reanalysis. The comparison has been performed from January to March 2012 and August 2012.

The accuracy of the wind speed derived from the HY-2A SCAT agree well with *in situ* wind observations and ECMWF reanalysis data, showing bias and RMSE of – 0.09 m s^{-1} and 2.02 m s^{-1} and 0.10 m s^{-1} and 1.81 m s^{-1}, respectively. However, the wind direction errors are a little higher. Overall, the lowest bias and RMSE of wind direction are – 1.78° and 28.92° for wind speed range of 5–10 m s^{-1} in open sea areas. Furthermore, the differences in wind speed between the two groups of comparison are wind speed dependent. The derived wind speeds are found to overestimate the buoy values at low-wind speeds (<5 m s^{-1}) and to underestimate at very high-wind speeds (>10 m s^{-1}). For the wind direction comparisons, the residual is almost zero except for a slight bias in lower (<4 m s^{-1}) and higher (>14 m s^{-1}) speed ranges. In addition, the accuracy is better for HY-2A SCAT wind products over the open sea compared with the coastal region.

Acknowledgements

The HY-2A wind speed products were obtained from the Chinese National Satellite Ocean Application Service (http://www.nsoas.gov.cn/NSOAS_En/index.html). The buoy wind data were downloaded from the NOAA/NDBC website (www.ndbc.noaa.gov). The ECMWF reanalysis data were downloaded from the ECMWF website (http://apps.ecmwf.int).

Funding

This work was supported by the Chinese Public Science and Technology Research Funds Projects of Ocean under Grant 201005009 and National Natural Science Foundation of China under Grant 41006112.

References

Bentamy, A., D. Croize-Fillon, and C. Perigaud. 2008. "Characterization of ASCAT Measurements Based on Buoy and Quikscat Wind Vector Observations." *Ocean Science* 4 (4): 265–274. doi:10.5194/os-4-265-2008.

Chi, C. Y., and F. K. Li. 1988. "A Comparative-Study of Several Wind Estimation Algorithms for Spaceborne Scatterometers." *IEEE Transactions on Geoscience and Remote Sensing* 26 (2): 115–121. doi:10.1109/36.3011.

Dong, X. L., K. Xu, H. G. Liu, and J. S. Jiang. 2004. "The Radar Altimeter and Scatterometer of China's HY-2 Satellite." *IGARSS 2004: IEEE International Geoscience and Remote Sensing Symposium Proceedings* 1–7: 1703–1706.

Ebuchi, N., H. C. Graber, and M. J. Caruso. 2002. "Evaluation of Wind Vectors Observed by Quikscat/Seawinds Using Ocean Buoy Data." *Journal of Atmospheric and Oceanic Technology* 19 (12): 2049–2062. doi:10.1175/1520-0426(2002)0192.0.CO;2.

Figa, J., and A. Stoffelen. 2000. "On the Assimilation of Ku-Band Scatterometer Winds for Weather Analysis and Forecasting." *IEEE Transactions on Geoscience and Remote Sensing* 38 (4): 1893–1902. doi:10.1109/36.851772.

Freilich, M. H. 1997. "Validation of Vector Magnitude Datasets: Effects of Random Component Errors." *Journal of Atmospheric and Oceanic Technology* 14 (3): 695–703. doi:10.1175/1520-0426(1997)0142.0.CO;2.

Katsaros, K. B., E. B. Forde, P. Chang, and W. T. Liu. 2001. "Quikscat's Seawinds Facilitates Early Identification of Tropical Depressions in 1999 Hurricane Season." *Geophysical Research Letters* 28 (6): 1043–1046. doi:10.1029/2000GL011646.

Large, W. G., J. Morzel, and G. B. Crawford. 1995. "Accounting for Surface-Wave Distortion of the Marine Wind-Profile in Low-Level Ocean Storms Wind Measurements." *Journal of Physical Oceanography* 25 (11): 2959–2971. doi:10.1175/15200485(1995)025<2959:AFSWDO>2.0.CO;2.

Lin, M., J. Zou, X. Xie, and Y. Zhang. 2013. "HY-2A Microwave Scatterometer Wind Retrieval Algorithm." *Chinese Engineering Sciences* 15 (7): 68–74. [In Chinese.]

Meindl, E. A., and G. D. Hamilton. 1992. "Programs of the National-Data-Buoy-Center." *Bulletin of the American Meteorological Society* 73 (7): 985–993. doi:10.1175/15200477(1992)0732.0.CO;2.

Satheesan, K., A. Sarkar, A. Parekh, M. R. R. Kumar, and Y. Kuroda. 2007. "Comparison of Wind Data from Quikscat and Buoys in the Indian Ocean." *International Journal of Remote Sensing* 28 (10): 2375–2382. doi:10.1080/01431160701236803.

Schultz, H. 1990. "A Circular Median Filter Approach for Resolving Directional Ambiguities in Wind Fields Retrieved from Spaceborne Scatterometer Data." *Journal of Geophysical Research-Oceans* 95 (C4): 5291–5303. doi:10.1029/Jc095ic04p05291.

Singh, R., P. Kumar, and P. K. Pal. 2012. "Assimilation of Oceansat-2-Scatterometer-Derived Surface Winds in the Weather Research and Forecasting Model." *IEEE Transactions on Geoscience and Remote Sensing* 50 (4): 1015–1021. doi:10.1109/TGRS.2011.2164410.

Sudha, A. K., and C. V. K. P. Rao. 2013. "Comparison of Oceansat-2 Scatterometer Winds with Buoy Observations over the Indian Ocean and the Pacific Ocean." *Remote Sensing Letters* 4 (2): 171–179. doi:10.1080/2150704x.2012.713140.

Wang, X. N., L. X. Liu, H. Q. Shi, X. L. Dong, and D. Zhu. 2012. "In-Orbit Calibration and Performance Evaluation of HY-2 Scatterometer." IEEE International Geoscience and Remote Sensing Symposium (Igarss), Munich, July 22–27, 4614–4616.

Wentz, F. J., and D. K. Smith. 1999. "A Model Function For the Ocean-Normalized Radar Cross Section at 14 GHz Derived from NSCAT Observations." *Journal of Geophysical Research-Oceans* 104 (C5): 11499–11514. doi:10.1029/98jc02148.